

A THEORETICAL STUDY OF STRUCTURE, BONDING AND PROPERTY OF PLATINUM(II)-8-HYDROXYQUINOLINE COMPLEXES WITH CARBENE AND HEAVIER HOMOLOGUES

Huynh Thi Phuong Loan¹, Hoang Van Duc², Nguyen Thi Ai Nhung^{1,*}

¹Department of Chemistry, University of Sciences, Hue University, 77 Nguyen Hue St., Hue, Vietnam

²Department of Chemistry, University of Education, Hue University, 34 Le Loi St., Hue, Vietnam

* Correspondence to Nguyen Thi Ai Nhung <ntanhung@hueuni.edu.vn>

(Received: 24 February 2020; Accepted: 18 March 2020)

Abstract. In this work, a theoretical study for platinum(II)-8-hydroxyquinoline-tetrylene complexes $[\{PtCl-C_9H_6NO\}-NHE_{Ph}]$ (Pt-EPh) is carried out for the first time by using the density functional theory (DFT). Quantum chemical calculations with DFT and charge methods at the BP86 level with basic sets SVP and TZVPP have been performed to get insight into the structures and property of Pt-EPh. The optimization of equilibrium geometries of the ligands EPh in Pt-EPh, bonded in the distorted end-on way to the Pt fragment is studied, in which the bending angle slightly decreases from carbene Pt-CPh to germylene Pt-GePh. Quantum chemical parameters such as E_{HOMO} , E_{LUMO} , the energy gap ($E_{LUMO} - E_{HOMO}$), electronegativity, global hardness, and global softness in the neutral molecules have been calculated and discussed. Bond dissociation energies decrease from the slighter to the heavier homologues. The hybridization of atoms E has large p characters, while the hybridization of atom Pt has a greater d character. Thus, the Pt-E bond possesses not only $NHE_{Ph} \rightarrow \{PtCl-C_9H_6NO\}$ strong σ -donation but also a significant contribution of π -donation $NHE_{Ph} \rightarrow \{PtCl-C_9H_6NO\}$, and a weak π -backdonation metal-ligand $NHE_{Ph} \leftarrow \{PtCl-C_9H_6NO\}$ in complexes Pt-EPh is also considered.

Keywords: tetrylene, bonding analysis, global softness, bond dissociation energy, platinum(II)-8-hydroxyquinoline

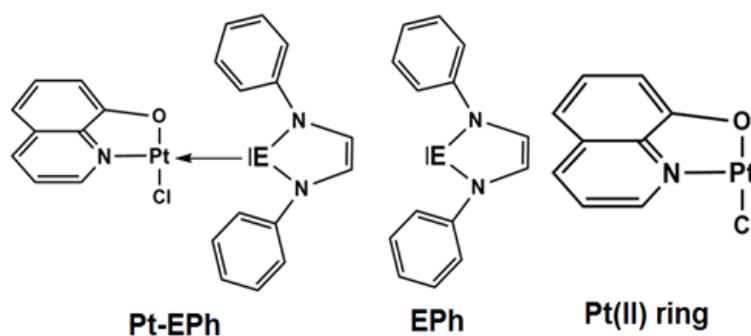
1 Introduction

In 1991, Arduengo [1] isolated an N-heterocyclic carbene (NHC) ligand in a stable form, which is a class of strong donor ligands with minimal π -back bonding from the metal center [2]. Particularly, distinct advantages that arise from the tight binding of the NHC ligand to the metal are derived from pre-catalysts. Thus, the greater stability of the complex under the catalytic conditions helps suppress the leading of the catalysts [3, 4]. In fact, NHC-based palladium, such as N-heteroaromatic-stabilized NHC-Pd(II) compounds, is well defined, including Pd-PEPPSI-NHC (PEPPSI = pyridine enhanced precatalyst preparation,

stabilization, and initiation), most notably used at high catalyst loadings [3, 5, 6]. Additionally, the PEPPSI catalyst, which has been shown to be very effective in catalyzing the coupling of sterically hindered chloroarenes, particularly with the Suzuki-Miyaura, Kumada-Tamao-Corriu, Buchwald-Hartwig, and Negishi coupling reactions [5, 7, 8]. Furthermore, the geometrical structures and nature of chemical bonding of complexes carrying carbene ligands NHC might exhibit a significant trend when versatile ligands NHCs connect with appropriate elements, and the properties have changed much when extending to the heavier homologues of NHE (E = Si→Pb) [9-13].

Besides, several organic compounds containing aromatic rings with one or more heteroatom sectors were used widely as corrosion inhibitors in industry and chemical sectors [14]. Consider that N-heterocycles are the most effective corrosion inhibitors among numerous inhibitors [15]. For instance, some N-heterocyclic compounds have been reported as good corrosion inhibitors for steel in acidic media, such as pyridine derivatives [16], pyrimidine derivatives [17], and pyridazine derivatives [18]. It is generally accepted that N-heterocyclic compounds exert their inhibition via adsorption on the metal surfaces through N-heteroatom, as well as those with triple or conjugated double bonds or aromatic rings in their molecular structures [19].

This paper provides results on the quantum chemical calculations of the structure and chemical bonding in complexes platinum(II)-8-hydroxyquinolines-tetrylene $[\{\text{PtCl-C}_9\text{H}_6\text{NO}\}\text{-NHE}_{\text{Ph}}]$ (Pt-EPh) (Scheme 1). This work aims to investigate the theoretically detailed structures and bondings of complexes Pt-EPh by using quantum chemical calculations. We calculated bond dissociation energies (D_e), Wiberg bond orders, natural partial charges, E_{HOMO} , E_{LUMO} , energy gap (ΔE), electronegativity (χ), global hardness (η), and global softness (S).



Scheme 1. Overview of platinum(II)-8-hydroxyquinolines-tetrylene complexes $[\{\text{PtCl-C}_9\text{H}_6\text{NO}\}\text{-NHE}_{\text{Ph}}]$ (Pt-EPh), NHE_{Ph} (EPh) (E = C, Si, Ge), and fragment Pt-ring investigated in this work

2 Computational details

The geometry optimizations of tetrylene complexes are performed with the BP86 [20, 21] functional in conjunction with the basis set def2-SVP by using the Gaussian 09 [22] and Turbomole 6.0.1 [23] programs. The Resolution of Identity (RI) approximation was used for all structure optimizations by using the appropriate auxiliary basis sets. All structures presented in this study are turned out to the minima on the potential energy surface (PES). The nature of the stationary points on the PES is confirmed as energy minima by means of frequency calculations. The bond dissociation energy (BDE – D_e , kcal/mol) is a measure of the strength of a chemical bond [24]. For instance, the bond dissociation energy for bond A–B, which is broken through reaction $\text{AB} \rightarrow \text{A} + \text{B}$ (25) of molecule AB and forms from two fragments E°_{A} and E°_{B} , is given by $\Delta E = E_{\text{AB}} - E^\circ_{\text{A}} - E^\circ_{\text{B}} = -D_e$. For bond dissociation energy calculation, the parent compounds and free ligands were firstly optimized at BP86/def2-TZVP. The level of theory at BP86/def2-TZVPP [26] //BP86/def2-SVP was used for the calculation of the BDEs by using the NBO 3.1 program [27] available in Gaussian 09.

To further explain the chemical bonding in complexes, the natural bond orbital (NBO) analysis is proposed to study the intermolecular interactions and apply to the analysis of bonding in complexes, particularly the charge transfer. The energetically lying occupied molecular orbitals were carried out for HOMO and LUMO orbitals of tetrylene complexes afterward [27]. Single point calculations with the same functional with geometry optimizations (BP86) but the larger def2-TZVPP basis set were carried out at the BP86/def2-TZVP geometries. In these calculations, the RI approximation was not used, and the level of theory is denoted as BP86/def2-TZVPP//BP86/def2-SVP and used for the calculation of the Wiberg bond orders and natural partial charges and also used for plotting molecular orbitals HOMO and LUMO, which have been analyzed by using the NBO method available in Gaussian 09.

Electron density distributions have been carried out by using bonding analysis. The HOMO energy (E_{HOMO}) indicates the tendency of the molecule to donate electrons. In contrast, the value E_{LUMO} of the molecules is lower, showing their more electron-accepting ability. The energy gap $\Delta E = E_{\text{LUMO}} - E_{\text{HOMO}}$ indicates the reactivity tendency of the organic molecule toward the metal surface with good inhibition efficiency. The ionization potential (I) and electron affinity (A) of the inhibitor molecules can be calculated through the application of Koopmans' theorem [28], which is related to HOMO and LUMO energy as: $I = -E_{\text{HOMO}}$ and $A = -E_{\text{LUMO}}$. The obtained ionization potential and electron affinity values were used to calculate the electronegativity (χ), global hardness (η), and global softness (S) of the molecule according to three following equations: $\chi = (I + A)/2$; $\eta = (I - A)/2$; $S = 1/\eta$.

3 Results and discussion

Figure 1 and Figure 2 present the optimized geometries of complexes Pt-EPh ($E = \text{C} \rightarrow \text{Ge}$) and free ligands EPh, together with the calculated values for the bond lengths and angles. Figure 1 shows that the Pt-C_{carbene} bond length is 1.976 Å. This bond length increases from Pt-CPh to Pt-GePh (2.354 Å). The NHE ligands in the complexes are bonded distorted end-on to the Pt-ring fragment with a bending angle of 178.2° in the carbene complex, and this angle slightly decreases in the silylene complex (177.8°) and germylene complex (177.3°). The E-N bonds in the parent complexes are slightly shorter than those in the free ligands EPh. Figure 2 also shows that the bond angles N-E-N in the complexes are more obtuse than those in the free ligands by 3–5°. Figure 1 also gives the calculated BDEs for the donor-acceptor bonds of Pt-EPh. The calculated BDEs suggest that the Pt-E bond strength decreases from Pt-CPh (69.3 kcal.mol⁻¹) to Pt-GePh (39.8 kcal.mol⁻¹). The data thus suggest that the heavier complexes have weaker bonds than the lighter adducts.

Furthermore, in Table 1, we report the quantum chemical parameters related to the molecular electronic structures of complexes Pt-EPh. The E_{HOMO} of Pt-EPh increases from -4.463 eV in Pt-CPh to -4.817 eV in Pt-GePh. This means that the electron-donating capability decreases in the following order: Pt-CPh > Pt-SiPh > Pt-GePh, and the capability of accepting electrons (E_{LUMO}) in Pt-EPh follows the similar order: Pt-CPh > Pt-SiPh > Pt-GePh. This leads to the decrease in energy gap ($\Delta E = E_{\text{LUMO}} - E_{\text{HOMO}}$) from carbene Pt-CPh to germylene Pt-GePh.

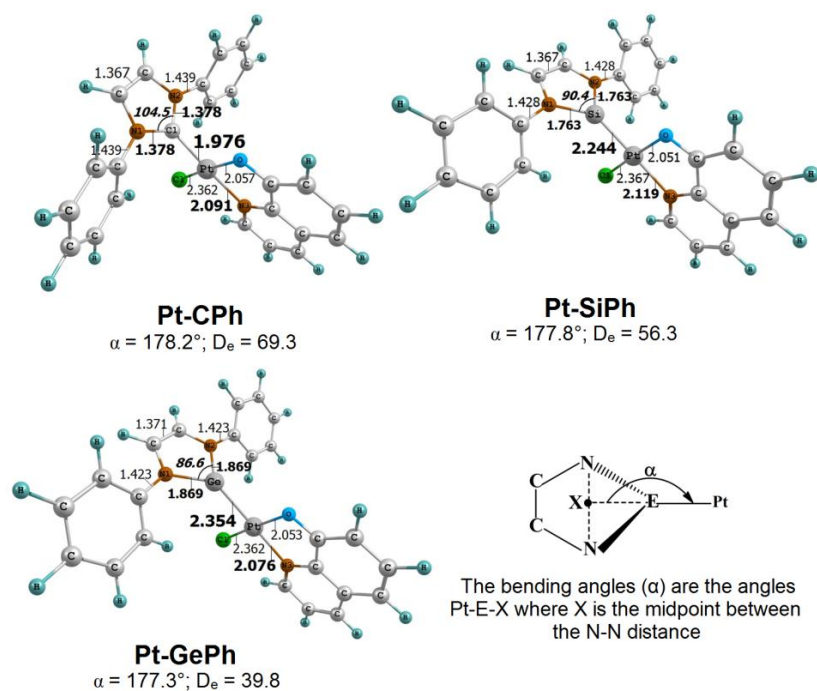


Fig. 1. Selected results (bond lengths in Å and angles in degrees) of optimized structures in Pt-EPh and fragment EPh at the BP86/def2-SVP level. Calculated BDEs, D_e (kcal.mol⁻¹) for Pt-EPh (E = C→Ge) at DFT-D_e-BP86/TZVPP level of theory

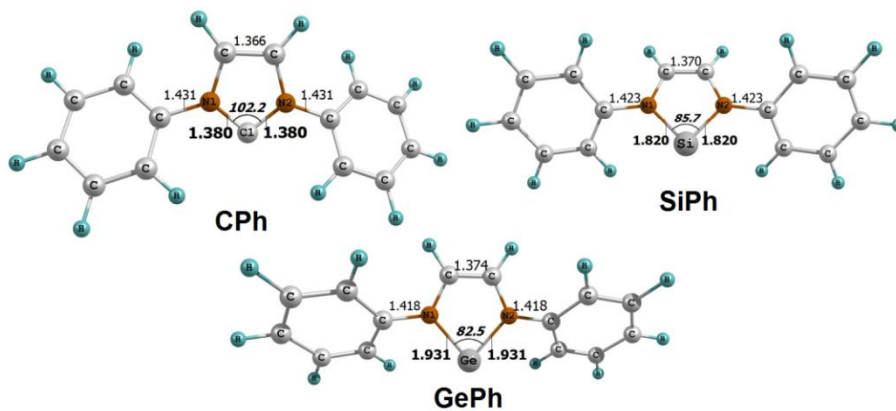


Fig. 2. Optimized geometries of ligands EPh (E = C, Si, Ge) at the BP86/def2-SVP level. Bond lengths are given in Å; angles in degrees

Table 1. Calculated quantum chemical parameters with ΔE_{GAP} (eV), ionization potential (I), electron affinity (A), electronegativities (χ), global hardness (η), and global softness (S) of complexes Pt-EPh (E = C, Si, Ge), obtained from the NBO data at the BP86/def2-TZVPP//BP86/def2-SVP level of theory

Complex	ΔE (eV) ($E_{\text{LUMO}} - E_{\text{HOMO}}$)	$I = -E_{\text{HOMO}}$	$A = -E_{\text{LUMO}}$	$\chi = (I + A)/2$	$\eta = (I - A)/2$	$S = 1/\eta$
Pt-CPh	1.905	4.463	2.558	3.511	0.953	1.049
Pt-SiPh	1.880	4.792	2.912	3.852	1.030	0.971
Pt-GePh	1.851	4.817	2.966	3.892	0.926	1.080

In addition, we plot MOs and orbital energy at the BP86/def2-TZVPP level of theory. The frontier molecular orbitals and orbital energy levels of the two occupied states of complexes Pt-CPh/Pt-GePh can be associated with σ - and π -types MOs in $[\text{PtCl-C}_9\text{H}_6\text{NO}]\leftarrow\text{NHE}_{\text{Ph}}$ with $E = \text{C} \rightarrow \text{Pb}$ (Figure 3). The energy levels of π -type donor orbitals of Pt-EPh are higher-lying than the σ -type donor orbitals. The HOMO-1 shows π -type symmetry for the silylene and germylene complexes, but the HOMO-5 exhibits π -orbitals for carbene Pt-CPh. The shape of the molecular orbitals indicates that the π donation from ligand to fragment $\{\text{PtCl-C}_9\text{H}_6\text{NO}\}$ might be important in the complexes. The HOMO-13 presents the σ -type MOs for adducts Pt-SiPh/Pt-GePh, while the higher-lying orbital energy levels belong to the lighter Pt-CPh with the HOMO-14 of the σ lone-pair orbitals. The analysis of the bonding shows that there is not only a strong interaction with the σ -lone pair of ligand EPh but also with the significant π -lone pair, in which the main Pt-E

bonds have strong σ -donation and a significant π -interaction.

The bonding of the free ligands reveals the highest-lying occupied MOs of the ligands EPh. The shape of the HOMO and HOMO-1 with σ - or π -symmetry is graphically shown in Figure 4. The HOMOs of NHE always have π -symmetry, while the HOMO-1 has σ -symmetry, except for the carbene complex. The shape of the π -HOMO clearly indicates that it is a lone-pair orbital. The largest coefficient of the σ -HOMO-2 and σ -HOMO is at atom E, but the participation of the NHE ring increases in heavier homologues. Thus, the shape of the HOMO-2 makes it perfectly suitable as a σ -donor orbital. The energies of the π -orbitals increase from C to Ge. The σ -orbitals are lower in energy than the π -orbitals and become lower in energy when E changes from C to Ge. The lower energy of the σ -lone pairs is due to the change to the tilted bonding of the ligands NHE [9].

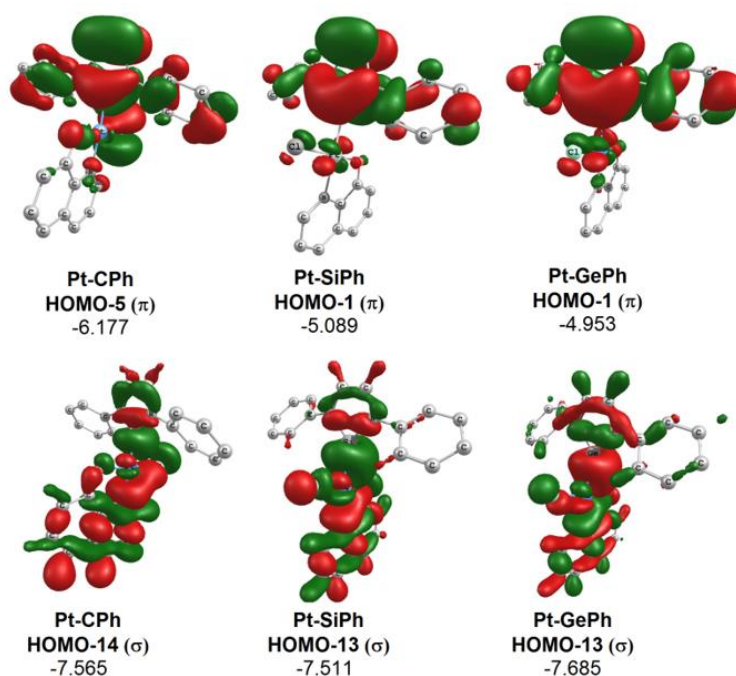


Fig. 3. MOs and orbital energy levels [eV] of σ - and π -types of the complexes Pt-EPh ($E = \text{C} - \text{Ge}$) at the BP86/def2-TZVPP level

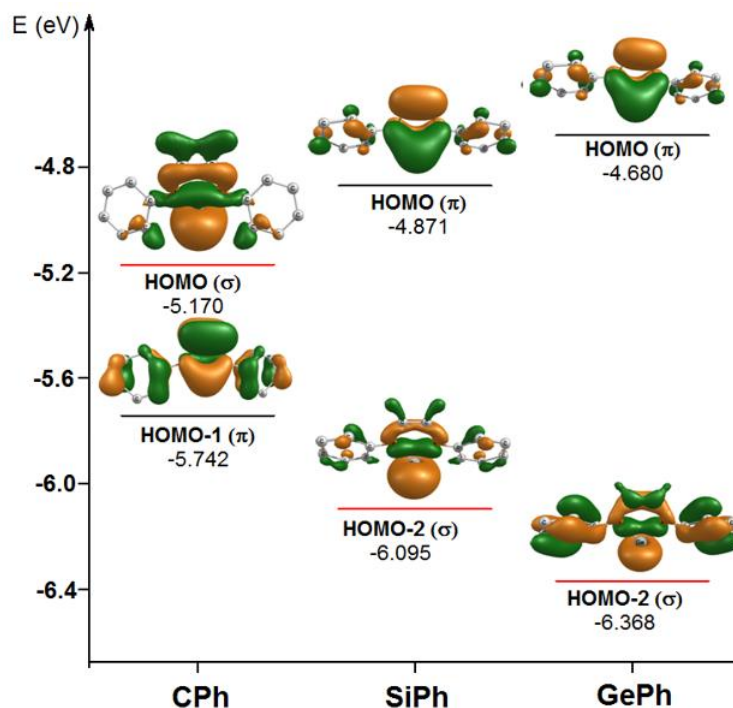


Fig. 4. Energy levels of the energetically highest lying σ and π orbital of free ligands

The polarization of the Pt–E σ -bonds in Pt–EPh and hybridization of the Pt–E bonds at atom E are shown in Table 2. The polarization of Pt–E bonds is strongly localized toward the E atom, and the p character of which is greater than 50%. The Pt–E bond in the distorted end-on-bonded tetrylene complexes Pt–EPh is mainly localized toward the carbon atom (63.6%), the silicon atom (52.9%), and the germanium atom (57.8%). The Pt–E bonds in Pt–EPh at atom E have a p character

increasing from 60.1% in Pt–CPh to 65.3% in Pt–SiPh, and *decreasing to* 56.2% in Pt–GePh. This is reasonable because σ and π donation Pt←NHE_{Ph} in the heavier complexes takes place from the σ and π lone-pair orbitals of the ligands EPh, which have a pure p character. Besides, the Pt–E bonds in Pt–EPh at atom Pt have an s character increasing from 21.1% in Pt–CPh to 26.3% in Pt–SiPh and from silylene complex to germylene complex (28.3%). However, the hybridization of d orbitals at atom Pt

Table 2. Polarization of the Pt–E σ bond and hybridization at atoms Pt and E from the NBO analysis of Pt–EPh (E = C, Si, Ge). The calculations were carried out at the BP86/def2-TZVPP//BP86/def2-SVP

Complex	Polarization		Hybridization				
	Pt–E		%s (E)	%p (E)	%s (Pt)	%p (Pt)	%d (Pt)
	% (Pt)	% (E)					
Pt–CPh	36.4	63.6	39.9	60.1	21.1	4.2	74.6
Pt–SiPh	47.1	52.9	34.6	65.3	26.3	7.7	65.9
Pt–GePh	42.2	57.8	43.7	56.2	28.3	11.2	60.3

also contributes more significantly to the carbene complex (74.6%) but slightly decreases from Pt–CPh to Pt–GePh (60.3%). Therefore, there exists a significant π -contribution from atom Pt to atom E of ligand EPh in complexes Pt–EPh. This might lead to a conclusion that the hybridization of atoms E and Pt has a large p character, while the hybridization of atom Pt has a greater d character, which clearly displays that the Pt–E bond possesses not only $\text{NHE}_{\text{Ph}} \rightarrow \{\text{PtCl}-\text{C}_9\text{H}_6\text{NO}\}$ strong σ -donation but also a great contribution of π -donation $\text{NHE}_{\text{Ph}} \rightarrow \{\text{PtCl}-\text{C}_9\text{H}_6\text{NO}\}$, and a π -backdonation metal ligand $\text{NHE}_{\text{Ph}} \leftarrow \{\text{PtCl}-\text{C}_9\text{H}_6\text{NO}\}$ in complexes Pt–EPh is also present in the distorted end-on-bonded tetrylene.

4 Conclusions

At an equilibrium structure, the slight ligands EPh and the tetrylene complexes Pt–EPh are bonded in the distorted end-on way to platinum(II)-8-hydroxyquinoline. The bond dissociation energies of Pt–EPh follow the order Pt–CPh > Pt–SiPh > Pt–GePh. The values of global softness are the lowest in Pt–SiPh and highest in Pt–GePh. The results of NBO analysis suggest that tetrylene ligands NHE_{Me} have strong σ -donation $\text{NHE}_{\text{Ph}} \rightarrow \text{Pt}$ and weak π -back-donation $\text{NHE}_{\text{Ph}} \leftarrow \text{Pt}$ in the $\text{NHE}_{\text{Ph}}-\text{Pt}(\text{II})$ interactions. The quantum chemical parameters, such as E_{HOMO} , E_{LUMO} , and the energy gap ($E_{\text{LUMO}} - E_{\text{HOMO}}$) in neutral molecules of system Pt–EPh, are localized over the N-heterocyclic tetrylene rings, which may reveal the active sites responsible for the active interaction of ligands with the metal fragment to form the versatile complexes oriented to the experimental study.

Funding statement

This research was funded by the National Foundation for Science and Technology Development (NAFOSTED) of Vietnam under grant number 104.06-2017.303.

Acknowledgments

Nguyen Thi Ai Nhung thanks Prof. Dr. Gernot Frenking for allowing the continued use of her resources within Frenking's group. The programs used in this study were run via the Annemarie cluster operated by Reuti (Thomas Reuter) at Philipps-Universität Marburg, Germany.

References

1. Arduengo III AJ, Harlow RL, Kline M. A stable crystalline carbene. *Journal of the American Chemical Society*. 1991;113(1):361-363.
2. Herrmann WA, Böhm VP, Gstöttmayr CW, Grosche M, Reisinger C-P, Weskamp T. Synthesis, structure and catalytic application of palladium (II) complexes bearing N-heterocyclic carbenes and phosphines. *Journal of Organometallic Chemistry*. 2001;617:616-28.
3. Poyatos M, Mata JA, Peris E. Complexes with poly (N-heterocyclic carbene) ligands: structural features and catalytic applications. *Chemical reviews*. 2009;109(8):3677-707.
4. Mata JA, Poyatos M, Peris E. Structural and catalytic properties of chelating bis- and tris-N-heterocyclic carbenes. *Coordination Chemistry Reviews*. 2007;251(5-6):841-59.
5. O'Brien CJ, Kantchev EAB, Valente C, Hadei N, Chass GA, Lough A, et al. Easily Prepared Air- and Moisture-Stable Pd–NHC (NHC= N-Heterocyclic Carbene) Complexes: A Reliable, User-Friendly, Highly Active Palladium Precatalyst for the Suzuki–Miyaura Reaction. *Chemistry–A European Journal*. 2006;12(18):4743-8.
6. Nasielski J, Hadei N, Achonduh G, Kantchev EAB, O'Brien CJ, Lough A, et al. Structure–Activity Relationship Analysis of Pd–PEPPSI Complexes in Cross-Couplings: A Close Inspection of the Catalytic Cycle and the Precatalyst Activation Model. *Chemistry–A European Journal*. 2010;16(35):10844-53.
7. Organ MG, Abdel-Hadi M, Avola S, Hadei N, Nasielski J, O'Brien CJ, et al. Biaryls made easy: PEPPSI and the Kumada–Tamao–Corriu reaction. *Chemistry–A European Journal*. 2007;13(1):150-7.

8. Organ MG, Avola S, Dubovyk I, Hadei N, Kantchev EAB, O'Brien CJ, et al. A User-Friendly, All-Purpose Pd–NHC (NHC= N-Heterocyclic Carbene) Precatalyst for the Negishi Reaction: A Step Towards a Universal Cross-Coupling Catalyst. *Chemistry–A European Journal*. 2006;12(18):4749-55.
9. Nguyen TAN, Frenking G. Transition-Metal Complexes of Tetrylones [(CO) 5W-E (PPh₃)₂] and Tetrylenes [(CO) 5W-NHE](E= C–Pb): A Theoretical Study. *Chemistry–A European Journal*. 2012;18(40):12733-48.
10. Frenking G, Tonner R, Klein S, Takagi N, Shimizu T, Krapp A, et al. New bonding modes of carbon and heavier group 14 atoms Si–Pb. *Chemical Society Reviews*. 2014;43(14):5106-39.
11. Frenking G, Hermann M, Andrada DM, Holzmann N. Donor–acceptor bonding in novel low-coordinated compounds of boron and group-14 atoms C–Sn. *Chemical Society Reviews*. 2016;45(4):1129-44.
12. Takagi N, Shimizu T, Frenking G. Divalent E (0) Compounds (E= Si–Sn). *Chemistry–A European Journal*. 2009;15(34):8593-604.
13. Takagi N, Frenking G. Divalent Pb (0) compounds. *Theoretical Chemistry Accounts*. 2011;129(3-5):615-23.
14. Moretti G, Guidi F, Grion G. Tryptamine as a green iron corrosion inhibitor in 0.5 M deaerated sulphuric acid. *Corrosion science*. 2004;46(2):387-403.
15. Bentiss F, Traisnel M, Gengembre L, Lagrenée M. Inhibition of acidic corrosion of mild steel by 3, 5-diphenyl-4H-1, 2, 4-triazole. *Applied Surface Science*. 2000;161(1-2):194-202.
16. Bouklah M, Ouassini A, Hammouti B, El Idrissi A. Corrosion inhibition of steel in 0.5 M H₂SO₄ by [(2-pyridin-4-ylethyl) thio] acetic acid. *Applied surface science*. 2005;250(1-4):50-6.
17. Zucchi F, TrabANELLI G, Brunoro G, Monticelli C, Rocchini G. Corrosion inhibition of carbon and low alloy steels in sulphuric acid solutions by 2-mercaptopyrimidine derivatives. *Materials and Corrosion*. 1993;44(6):264-8.
18. Chetouani A, Aouniti A, Hammouti B, Benchat N, Benhadda T, Kertit S. Corrosion inhibitors for iron in hydrochloride acid solution by newly synthesised pyridazine derivatives. *Corrosion Science*. 2003;45(8):1675-84.
19. Umoren S, Obot I. Polyvinylpyrrolidone and polyacrylamide as corrosion inhibitors for mild steel in acidic medium. *Surface Review and Letters*. 2008;15(03):277-86.
20. Becke AD. Density functional calculations of molecular bond energies. *The Journal of Chemical Physics*. 1986;84(8):4524-9.
21. Lee C, Yang W, Parr RG. Development of the Colle-Salvetti correlation-energy formula into a functional of the electron density. *Physical review B*. 1988;37(2):785.
22. G. Gaussian Inc. In: Frisch MJ TG, Schlegel HB, Scuseria GE, Robb MA, Cheeseman JR, Scalmani G, Barone V, Mennucci B, Petersson GA, editors. Wallingford CT; 2009.
23. Ahlrichs R, Bär M, Häser M, Horn H, Kölmel C. Electronic structure calculations on workstation computers: The program system turbomole. *Chemical Physics Letters*. 1989;162(3):165-9.
24. Szwarc M. The Determination of Bond Dissociation Energies by Pyrolytic Methods. *Chemical Reviews*. 1950;47(1):75-173.
25. Kerr J. Bond dissociation energies by kinetic methods. *Chemical reviews*. 1966;66(5):465-500.
26. Weigend F, Ahlrichs R. Balanced basis sets of split valence, triple zeta valence and quadruple zeta valence quality for H to Rn: Design and assessment of accuracy. *Physical Chemistry Chemical Physics*. 2005;7(18):3297-305.
27. Reed AE, Weinstock RB, Weinhold F. Natural population analysis. *The Journal of Chemical Physics*. 1985;83(2):735-46.
28. Lukovits I, Kalman E, Zucchi F. Corrosion inhibitors—correlation between electronic structure and efficiency. *Corrosion*. 2001;57(1):3-8.